Development of a method for fast crack testing of high-grade polymers

J. P. DEAR
Department of Mechanical Engineering, Imperial College of Science, Technology and Medicine, Exhibition Road, London SW7 2BX, UK

A technique is described which takes advantage of the good thermal insulation properties of polymers and their tendency to become embrittled when cooled to low temperatures and so make crack initiation in an embrittled part of a specimen a simple process. In many tests, the practice is to initiate a crack in a specimen of polymer or similar material by using an impacting device that also applies dynamically a three-point bend. A problem with this approach can be in determining how much the crack initiation and propagation is due to the strong transient forces relative to the bending or other dynamic loading. As the toughness, dynamic and other properties of materials are improved and hence higher impact velocities are required, so this factor becomes more difficult to resolve. Thus, there is increasing interest in different arrangements for testing these new materials that avoid transient impact problems, and also to provide better information concerning the threshold load for crack propagation and related factors. On-specimen gauges are used for some of these studies.

1. Introduction

There is now much interest in the propagation of cracks in a polymer under well-defined steady stress conditions that are kept free of impact, shock or other crack-launching transient forces. This is particularly so for thin sheets of material in the order of 3 to 4 mm thickness and when the threshold between slow and fast crack propagation needs to be carefully defined. Much higher quality materials are now becoming available in sheet form, for high stress applications, so the need for this type of testing is on the increase. A particular problem is to find a test method whereby a sheet of material can be first loaded and then allowed to stress relax to a well-defined level before a crack is initiated. Unwanted are impacts or other crack initiation techniques which can unduly disturb the steady-state stress conditions that have been carefully created in the specimen. A problem with such impact techniques is the transient forces they generate [1–3]. These complex forces then sweep through the specimen, not only making stress levels difficult to determine but also influencing and sometimes dominating the crack propagation processes [4–10]. For example, partial crack arrest lines, varying areas and degrees of micro-ductility, crack tip blunting and other factors need to be explained which can be much in evidence near to the threshold of slow to fast crack propagation in a specimen.

A test method is presented in this paper which is particularly suitable for thin sheet specimens and meets the test conditions outlined above. A rectangular specimen with a tongue protruding from one side is taken from the sheet material to be assessed. This protruding tongue of material with the crack path through its centre is quickly frozen using liquid nitrogen, or other agent, to take the tongue material well into its brittle phase. As polymers are good insulators, it is possible to do this without significant, if any, cooling of the main specimen material. Before freeze cooling of the tongue material, the main specimen is loaded in a direction normal to the intended crack path. If required, a controlled amount of stress relaxation can be introduced. Initiating the crack in the tongue is very simply achieved using a static three-point bend device. The fast crack in the tongue of the material on reaching the main part of the specimen will either be slowed down and arrested or achieve a slow or fast crack to sever the specimen depending on the strength of the stress field. In this way, the threshold of fast crack propagation in the material can be established and also how crack velocity varies with intensity of the stress field in the main part of the specimen. On-specimen strain gauges were used to monitor the progress of the crack and to observe crack tip stress intensities.

2. Experimental procedure

The specimens used in this research are illustrated in Fig. 1. In all cases, the tongue of the specimen was side-grooved to guide the crack into the specimen. Mostly, the main section of the specimen was also side-grooved for more precise measurement of the slow to fast crack propagation conditions. A few specimens were not side-grooved in order to observe the forking of a free-running crack and sites exhibiting the "rabbit-ear" shaped depressions at 45°. Results
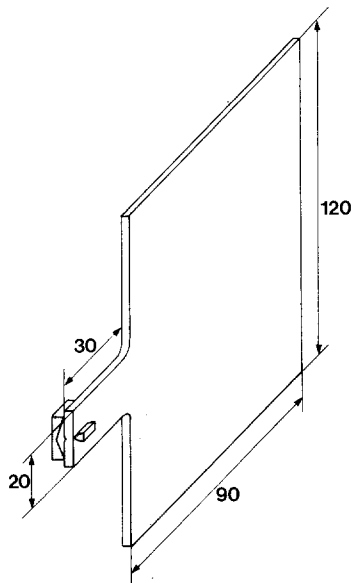
Figure 1 Specimen geometry showing the height, *H* (120 mm), and width, *W* (90 mm), of test section with dimensions of tongue (20 mm × 30 mm); thickness, *B* (3 mm), and side-groove depth, 0.5 mm. Also, shown is an illustration of the shallow angle (10°) static three-point bend device.

are presented for polyethylene sheet (nominally 3 to 4 mm) of different grades.

A jig was made to hold securely the specimen in an Instron machine and to load uniformly the specimen in the direction normal to the intended crack path. After loading the specimen, the Instron cross-head was stopped and the specimen allowed to stress relax down to a chosen value. Meanwhile, the point of the tongue furthest from the main section of the specimen was freeze cooled with liquid nitrogen using vessels described below. A fast crack in the tongue was initiated using a static three-point bending device as illustrated in Fig. 1. This procedure, as well as providing for stress equalization in the specimen before crack generation, also meant that the timing of the crack initiation was not difficult as the rate of stress relaxation had much reduced.

The experiments were repeated for a range of loading and relaxation stress times to identify the threshold of slow to fast cracking of the main section of the specimens. Several different grades of polymers were tested in this way. High-speed framing photography employing an image-converter IMACON camera was used to observe the generation and passage of the cracks through the specimen. For this, the specimen was illuminated from behind using Monolite (50J) flash units so that the specimen appeared as a dark shadow in the photographs and the crack as a bright streak of light. Synchronization was achieved by the breaking of a thin conducting strip at the beginning of the crack path in the main section of the specimen.

Several vessels were made to hold the liquid nitrogen. These vessels had slots in one side for the tongue of the specimens to enter the vessel prior to it being filled with nitrogen. The different types of nitrogen vessels provided for the specimens to be

tested in the vertical or horizontal plane and for different volumes of nitrogen to be held to suit different thicknesses of specimen. The slots through which the specimen tongue entered the vessels were provided with a packing gland to make sealed joints. Expanded polystyrene was used to insulate the inside of these vessels. With experimental care, these simple test facilities provided consistent results. Of course, there is scope to refine these techniques to provide for a more routine procedure with better timing control and other improvements.

Prior to the experiments, it was established that the thermal front would be in the tongue or just entering the main section of the specimen when the crack was initiated depending upon the sample dimensions and other test conditions. This was assessed by fully inserting the tongue of a polymer specimen into a nitrogen vessel so that most of the tongue was brittle-cooled. Using thermocouples, the temperature was monitored at the 10, 20 and 30 mm points along the crack path into the main section of the specimen. In the fracture experiments, the time to freeze the tongue and to initiate the crack was approximately 60 sec. In the thermocouple test, in 60 sec, the temperature at the 10, 20 and 30 mm points fell by 2, 1.4 and 0.5 °C, respectively. This relates to an increase of modulus of the order of 7%, 3.5% and 1.8% at these points. This being a worst case possibility because in the experiments, as stated above, only the end half of the tongue was inserted into the nitrogen vessel. Thus, for the experiments presented in this paper, there would only be a very small increase in modulus at the beginning of the 90 mm crack path length in the main section of the specimen. This would coincide with the build up of stress from no load in the tongue to the crack seeing the full load in the main section of the specimen.

A simple method has been devised and used to illustrate the distribution of strain at the root of the tongue when it joins the main specimen. A grid of squares was printed on to the surface of a sheet of low-modulus (∼ 10 MPa) viscoelastic material in the shape of the polymer test specimen used in the experiments. The low-modulus model was stressed uniaxially in the same way as the polymer specimens. Fig. 2 shows that the strain distortion in the low-modulus model extends from the root of the tongue
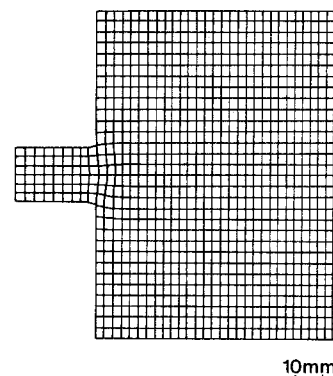
10mm

Figure 2 Strain distribution in the specimen.

322

into the main section of the specimen for ~ 10 mm and thereafter the strain pattern has equalized. A low-modulus model was used because this would show a greater strain distortion and hence redistribution of stress than the stiffer polymer materials having a modulus greater than 800 MPa.

3. Results

The results presented in this paper are for high-density polyethylene (HDPE) and medium-density polyethylene (MDPE). Crack propagation through the specimens is related to force–time loading curves using the load sensor in the Instron and also from sensors placed on the specimen.

3.1. HDPE samples

There was very little difficulty in repeating the tests, once the timing of the stressing of the specimen and freeze-time of the specimen had been determined. Indications were that the variability due to experimental procedure was much less than the variation in the properties of the material and thickness dimensions of the samples. As is to be expected, the higher the test stress levels applied to the specimen, the faster the crack propagation.

Fig. 3b shows a high-speed photographic sequence of eight frames of crack propagation in a HDPE
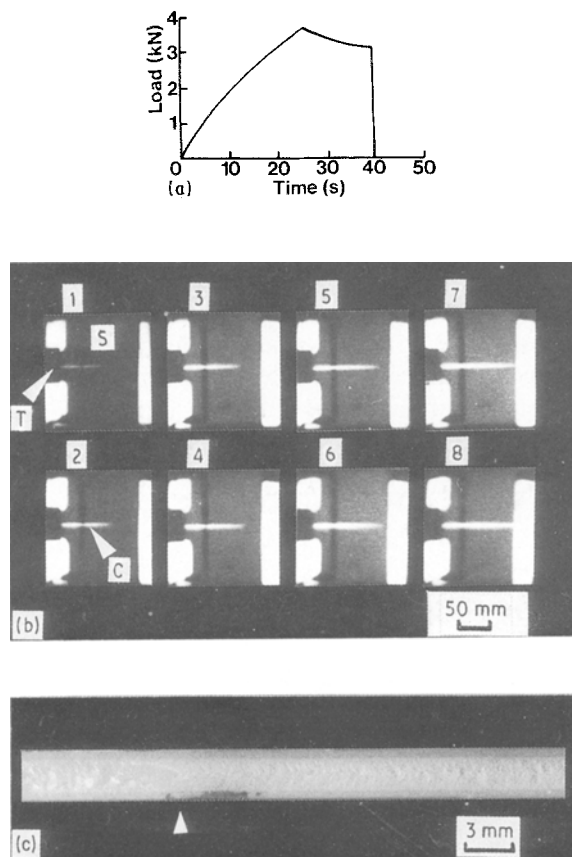
specimen. The specimen is backlighted and so appears black against a white background. The tongue is on the left. The white horizontal line which forms in frame 2 is the crack. Using these photographs, the average crack velocity was measured as ~ 300 m sec^{-1}. Fig. 3a is a force–time trace which shows that as the Instron extended the specimen at a constant rate, the stress build up in the specimen followed an exponential curve. When the load applied to the specimen reached 3.72 kN the Instron cross-head was stopped. The stress in the specimen then began to exponentially decay and by the time the load had reduced to 3.23 kN, the stress relaxation rate had levelled off and generally there was a good equalization of stress in the specimen. At this instant, the crack was initiated. During the early stress relaxation in the specimen and before crack initiation, the tongue of the specimen was cooled with liquid nitrogen so that a crack could easily be started in the tongue with the static three-point bend device. Very noticeable in the photograph of the fracture surfaces, in Fig. 3c, is that they are free of partial arrest lines and have a good even distribution of micro-ductility and other features along the whole length of the crack surfaces.

The above experiment was repeated using a different sample from the same sheet of HDPE material but applying a lower peak loading of 3.23 kN and a stress relaxed loading of 2.65 kN before cracking the specimen. The crack velocity for this lower stress level in the specimen was ~ 160 m sec^{-1} which is about one half of the velocity when the peak loading was 3.72 kN. Again the fracture surfaces showed no indication of partial arrest. For several such tests, similar smooth fracture surfaces were obtained.

A lower peak loading of 2.94 kN and stress relaxed to a load of 2.45 kN resulted in a lower crack velocity of ~ 70 m sec^{-1} with crack arrest just before the specimen was severed. The test conditions for this experiment are clearly near to the threshold between slow to fast cracking of the specimen. Fig. 4 is a plot of crack velocity against the stress relaxed load for six HDPE experiments including the three described above. Some of the tests at the lower crack velocities were repeated and the same results were obtained.

3.2. MDPE samples

A similar set of experiments was conducted on MDPE samples and an example is presented in Fig. 5. For these tests on the tougher MDPE material, slightly higher loads were used. The main points to emerge were that the crack velocities were much lower though the results had much the same form and pattern as before. Fig. 6 shows the crack velocity data plotted against stress relaxed load. An additional point was that the separation of the fracture surfaces after they had been severed by the crack, D_f, was greater for the MDPE than for the HDPE namely a gap of ~ 2 mm for MDPE and ~ 1 mm for HDPE samples. Data for MDPE and HDPE samples are presented in Table I which are for the tests referred to above. To be consistent, the gap was measured at the centre of the crack path.

Figure 3 HDPE specimens. (a) Force–time loading curve for stress-relaxed load of 3.23 kN. (b) High-speed photographic sequence (interframe time 20 μsec): T, tongue; S, specimen; C, crack. (c) A section of the fracture surface showing the transition (see arrow) from frozen tongue to the smoother main section of the specimen.
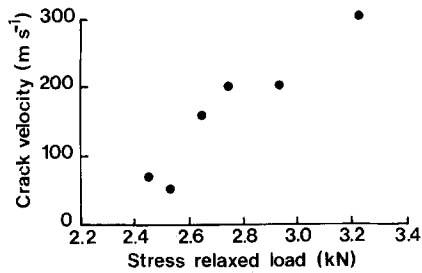
Figure 4 Plot of crack velocity against stress-relaxed load for HDPE specimens tested.
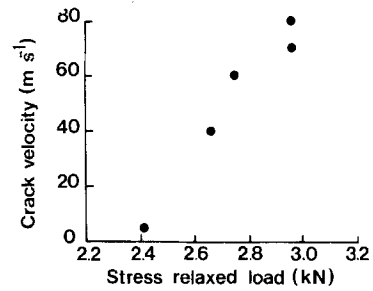
Figure 6 Plot of crack velocity against stress-relaxed load for MDPE specimens tested.
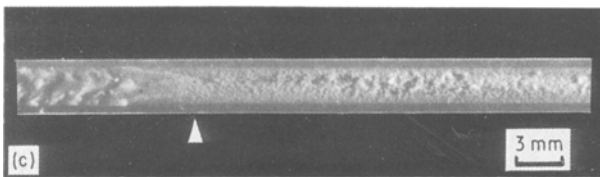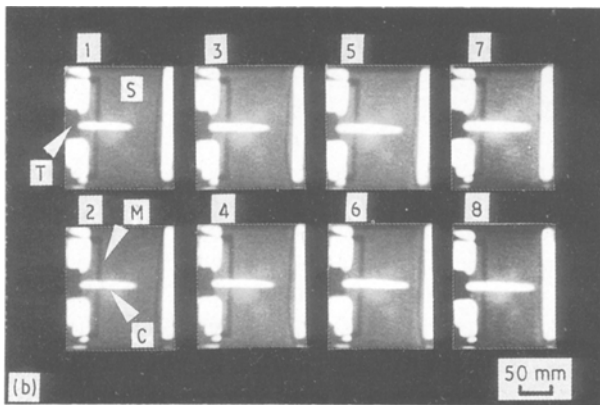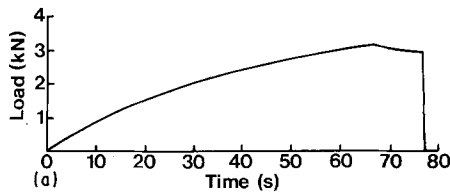
Figure 5 MDPE specimens. (a) Force–time loading curve for stress relaxed load of 2.94 kN. (b) High-speed photographic sequence (interframe time 40 μsec): T, tongue; S, specimen; C, crack; M, metallic trigger-strip. (c) A section of the fracture surface showing the transition (see arrow) from frozen tongue to the smoother main section of the specimen.

3.3. Free-running cracks

Some specimens were tested without side-grooves partly as a check that the side-grooves were not essential to achieve a failure of a specimen under these experimental conditions and also because there is a research interest in how free-running cracks would behave when propagating in a unidirectional stress field. Fig. 7 is a photograph of a specimen with a free-running crack. It starts off as a fast crack with little sign of any surface depression at the edge of the crack. There is a tendency for the crack to zig-zag as it generally follows a path normal to the stress field. This is until a point is reached when the crack divides into two with one crack either side of the path normal to the stress field (see Field [3]). Soon after, both cracks are arrested with increasing surface depression of material at the crack tip and a well-defined "rabbit-ear" formation. Several tested specimens showed very much the same crack behaviour and there may well be more to be learnt about possible links between the zig-zag deviations of the fast crack, the division of the main crack into two and then the "rabbit-ear" arrest.

3.4. On-specimen strain gauges

With regard to energy flow into the crack tip, models have been developed using simple lumped constants of mass, stiffness and viscous friction or electrical analogues [11–13]. It is clearly important to attempt to test such models experimentally. Fig. 8 shows the type of results that can be obtained if strain gauges are attached to specimens. These results are for HDPE specimens and the on-specimen strain gauge was located about half-way along the crack path and a little

TABLE I Tabulation of the peak load, stress-relaxed load, crack velocity and the separation of the fracture surfaces after test, D_f, for HDPE and MDPE samples

Material	Peak load (kN)	Stress-relaxed load (kN)	Crack velocity (m sec^{-1})	D_f (mm)
HDPE	3.72	3.23	300	1.5
HDPE	3.23	2.65	160	1.2
HDPE	2.94	2.45	70[a]	0.75
MDPE	3.14	2.94	80	2.5
MDPE	2.93	2.74	60	2.0
MDPE	2.74	2.65	40[a]	1.25

[a] Crack arrested.

324
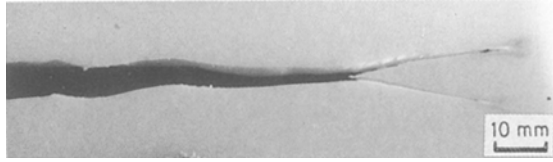
Figure 7 Free-running crack showing "rabbit-ear" depression at arrested crack tip.
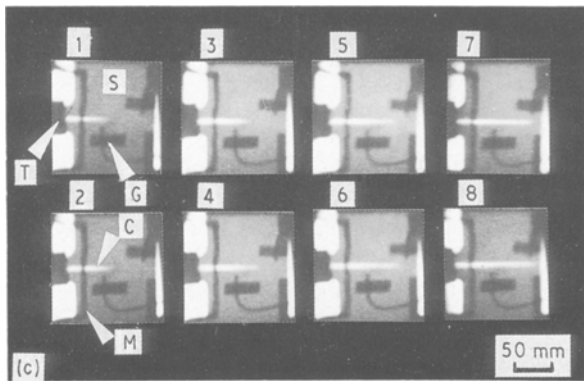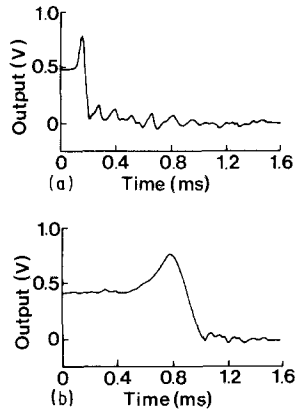
Figure 8 (a) Strain gauge output for HDPE specimen fractured at 2.74 kN. (b) Strain gauge output for HDPE specimen fractured at 2.54 kN. (c) High-speed photographic sequence (interframe time 40 μsec) showing position of strain gauge (G), tongue (T), specimen (S), crack (C) and a metallic trigger-strip (M).

distant from it. The aim was to monitor the intensity of stress at the crack tip as it passed the strain gauge monitor. The results show this well with the stress constant until the crack tip passes to one side of the strain gauge when the stress level increases to a peak and then quickly falls away as the crack tip moves away from the gauge. For the first test (Fig. 8a), the stress-relaxed loading was 2.94 kN and the crack velocity was ~ 200 m sec^{-1}. For Fig. 8b, a lower stress-relaxed loading of 2.54 kN was used to achieve a slower crack velocity. The force–time trace obtained from the on-specimen strain gauge, therefore has a longer delay before the crack tip passes by the strain gauge to produce a longer rise and fall impulse. A high-speed photographic sequence (Fig. 8c) shows the crack passing by the strain gauge and this was also used to obtain crack-velocity measurements. There are, of course, a variety of studies that can be performed using on-specimen strain gauges to study more

fully crack tip stress intensity effects and the variation in crack velocity for changing stress loading along the crack path length. On-specimen strain gauges have also been used for studying the transient effects of impact initiation of fracture of materials (see [14]) and some interesting comparisons can be made between these impact tests and those reported on in this paper.

4. Discussion
4.1. Determination of K and G
The experimental information obtained provides for several analytical calculations and for development of models. Perhaps, two of the more important calculations are for K and G and it is these which are given below. In the presented experiments, the crack is primarily driven by the flow of available elastic energy stored in the specimen. In practice, it will take a finite time for available strain energy to flow into the crack tip. However, in the present analysis the flow is considered to be instantaneous.

If it is assumed that all the elastic energy is absorbed by the crack then the following gives the value of G_s [11]

$$G_s = (P_0^2 H / 2EB^2 W^2)(B/B_N)^2 \qquad (1)$$

where P_0 is the minimum stress relaxed load for fast fracture, E is the dynamic modulus of elasticity (2.2 GPa for HDPE and 1.8 GPa for MDPE) and the factor $(B/B_N)^2$ is included because of the use of side-grooves to ensure an in-plane fracture path in the specimen. For a HDPE sample when the crack only just severs the specimen, this gives a G_s of approximately 5.0 kJ m^{-2}. For a MDPE sample, again, when the crack only just severs the specimen, this gives a G_s of approximately 7.2 kJ m^{-2}. Similar values for G_s were obtained using the following expression

$$G_s = (P_0 D_f / 2BW)(B/B_N) \qquad (2)$$

where D_f is the displacement of the fracture surfaces measured after the test. These being for HDPE a G_s of 5.1 kJ m^{-2} and for MDPE a G_s of 9.2 kJ m^{-2}. It follows that the higher the elastic energy then the faster can be the crack propagation and also the greater the residual energy that is not expended in producing crack surfaces.

The experimental data obtained from on-specimen sensors provides for a different and interesting way of arriving at the stress concentration at the crack tip. For example, the on-specimen strain–time trace shows a rise of strain as the crack tip passed the strain gauge. This rise is of the order of 50%. The strain gauge was well away from the edges of the specimen so the distribution of stress would be near to that for an infinitely large specimen. Using the Irwin stress function solutions

$$\sigma_{ij} = [K/(2\pi r)^{1/2}] f_{ij}(\theta) \qquad (3)$$

the stress intensity factor K can be estimated using the following expression

$$K = 0.94(1.5P/BW)(2\pi r)^{1/2} \qquad (4)$$

where r is the distance of the strain gauge from the

325

crack tip and the peak stress at the strain gauge is noted to be 50% greater than the mean stress. For the HDPE sample, in Fig. 8, this gives a stress intensity at the crack tip of $\sim 3.5\ \mathrm{MPa\,m^{1/2}}$. It is interesting to place several strain gauges at equal distance from the crack path. It is then possible to measure the reducing crack intensity peak and other stress levels as energy is absorbed to create crack surfaces at different crack velocities. It is planned to present this research in another paper.

4.2. Crack velocity

It is interesting to link the findings of this experimental study with the model derived by Williams [11] which represents a sample of polymeric material as a lumped mass-spring system. Such models can be derived for cracks propagating through sheets of material that provide for an infinite crack path length. This is such that the crack tip always sees a constant stress field and the same availability of strain energy. For crack paths of finite length then care is needed in adjusting the modelling terms and this is particularly so for very short path lengths. However, for the specimen dimensions used for these experiments, it is interesting to note that there is quite a good fit between experimental data and the Williams' spring mass models for a specimen in uniaxial tension. The expression for the crack velocity, $\mathrm{d}a/\mathrm{d}t$, in this model is

$$\mathrm{d}a/\mathrm{d}t = C_m[1 - (P_0/P)^2]^{1/2} \qquad (5)$$

where P_0 is the threshold stress-relaxed load for crack propagation, P the stress relaxed load applied to the specimen and C_m is the maximum value of crack velocity attainable. Employing regression analysis (see Fig. 9) to fit the experimental data to the prediction model gives for HDPE, $P_0 = 2.46\ \mathrm{kN}$ and $C_m = 440\ \mathrm{m\,sec^{-1}}$ (this gives a G_s of $5.1\ \mathrm{kJ\,m^{-2}}$) and for MDPE, $P_0 = 2.43\ \mathrm{kN}$ and $C_m = 130\ \mathrm{m\,sec^{-1}}$ (this

gives a G_s of $6.1\ \mathrm{kJ\,m^{-2}}$). The sample correlation coefficients are 0.938 and 0.943 for the HDPE and MDPE samples, respectively. The experimental techniques developed in the present work, which allow both crack velocity and strain energy to be monitored, have great potential for assessing theoretical models of crack growth.

5. Conclusion

The main aim of this paper has been to introduce a new experimental technique for studies of crack propagation in sheet polymer material and specimens of other dimensions. The technique can be used for a variety of materials that are inherently good insulators so that the tongue projecting from one side of a specimen can be freeze cooled to take it into its brittle state without significantly affecting the bulk of the test specimen. The tongue is largely isolated from the stressing of the main specimen section so that the crack produced in the tongue is free running until it reaches the main section of the specimen. In these experiments, the specimen was uniaxially stressed but other specimen configurations and stress states are possible.

Research is proceeding with specimens at different temperatures and using on-specimen sensors in a variety of ways. This includes studying crack propagation through bonded joints, changing section of material and a variety of other such features. It is thought that the crack propagation technique presented, as well as being a versatile research tool, could be developed into a standard test method for polymer and similar materials including composites.

Figure 9 Experimental data fitted to Equation 5 for (a) HDPE specimens, and (b) MDPE specimens.

References
1. H. SCHARDIN, "Velocity effects in fracture" in "Fracture", edited by B. L. Averbach, D. J. K. Fellbeck, G. T. Hahn and D. A. Thomas (Wiley, New York, 1959) Ch. 16.
2. H. KOLSKY, "Stress Waves in Solids" (Clarendon Press, Oxford, 1953).
3. J. E. FIELD, *Contemp. Phys.* 1 (1971) 31.
4. J. G. WILLIAMS, "Fracture Mechanics of Polymers" (Ellis Horwood, Chichester, 1984) Ch. 8.
5. J. G. WILLIAMS and J. M. HODGKINSON, *Proc. R. Soc. London* A 375 (1981) 231.
6. A. J. KINLOCH, G. A. KODOKIAN and M. B. JAMARANI, *J. Mater. Sci.* 22 (1987) 4111.
7. J. F. KALTHOFF, W. BOHME, S. WINKLER and W. KLEMM, in "Proceedings of 5th International Conference on Fracture", Cannes, Vol. 1, edited by D. Francois (Pergamon, Oxford, 1985) p. 363.
8. D. IRELAND, in "Proceedings of International Conference on Dynamic Fracture Toughness", edited by M. G. Dawes (Welding Institute, London, 1976).
9. J. P. DEAR, *J. Appl. Phys.* submitted.

10. J. G. WILLIAMS and R. M. S. GENUSSOV, *Int. J. Fract.* **38** (1988) R9.
11. J. G. WILLIAMS, *ibid.* **33** (1987) 33.
12. J. G. WILLIAMS and G. C. ADAMS, *ibid.* **33** (1987) 209.
13. B. A. CROUCH and J. G. WILLIAMS, *J. Mech. Phys. Solids* **36** (1988) 1.
14. J. P. DEAR and J. H. MacGILLIVRAY, *J. Mater. Sci.* submitted.